Suppression of chromosome instability limits acquired drug resistance

Elizabeth A Crowley[1], Nicole M Hermance[1], Conor P Herlihy[1], Amity L Manning[1*]

[1] Department of Biology and Biotechnology, Worcester Polytechnic Institute, Worcester, MA, 01609 USA

[*]Corresponding author:
Amity L Manning
Email: almanning@wpi.edu
tel: 508-831-4961

The authors declare no potential conflicts of interest.

Key words:
Mitosis, genomic instability, Aurora B, Gefitinib, NSCLC

Running Title: Suppression of CIN limits drug resistance

Statement of Significance:

Modulation of microtubule dynamics in cells that exhibit chromosome instability (CIN) is sufficient to promote mitotic fidelity, reduce genomic heterogeneity, and limit acquisition of drug resistance.

Abstract:

Numerical chromosome instability, or nCIN, defined as the high frequency of whole chromosome gains and losses, is prevalent in many solid tumors. nCIN has been shown to promote intra-tumor heterogeneity and corresponds with tumor aggressiveness, drug resistance and tumor relapse. While increased nCIN has been shown to promote the acquisition of genomic changes responsible for drug resistance, the potential to modulate nCIN in a therapeutic manner has not been well explored. Here we assess the role of nCIN in the acquisition of drug resistance in non small cell lung cancer. We show that generation of whole chromosome segregation errors in non small cell lung cancer cells is sensitive to manipulation of microtubule dynamics and that enhancement of chromosome cohesion strongly suppresses nCIN and reduces intra-tumor heterogeneity. We demonstrate that suppression of nCIN has no impact on non small cell lung cancer cell proliferation *in vitro* nor in tumor initiation in mouse xenograft models. However, suppression of nCIN alters the timing and molecular mechanisms that drive acquired drug resistance. These findings suggest mechanisms to suppress nCIN may serve as effective co-therapies to limit tumor evolution and sustain drug response.

Introduction

Whole chromosome instability, or numerical CIN (nCIN), is generated by underlying defects in mitosis [1, 2]. The aneuploidy that results from mitotic segregation errors promotes intra-tumor heterogeneity and is a driving force in cancer that contributes to tumor evolution and drug resistance [1-7]. Chromosome segregation is exquisitely sensitive to the regulation of dynamic microtubule attachments and defects that either increase or decrease the stability of microtubule attachments can corrupt mitotic fidelity and contribute to nCIN [8, 9]. Conversely, perturbations that reduce nCIN are proposed to limit acquired drug resistance and may hold therapeutic potential.

Aurora B kinase is a master regulator of kinetochore-microtubule dynamics during mitosis. Its overexpression is common in many cancer contexts and recent analyses of over 10,000 cancer genomes from the Cancer Genome Atlas show that, across cancer subtypes, Aurora B expression corresponds with degree of aneuploidy [10]. Increased expression of Aurora B also correlates with poor patient prognosis in a variety of cancer contexts [11]. Aurora B is a component of the Chromosome Passenger Complex (CPC). The CPC localizes to the centromere where Aurora B kinase activity regulates localization and activity of numerous kinetochore components responsible for binding and stabilizing kinetochore microtubule attachments, thereby promoting satisfaction of the spindle assembly checkpoint and regulating chromosome segregation [12]. Consistent with this function, both decreased and increased Aurora B activity at the centromere results in chromosome segregation errors [13-18].

Here we demonstrate that in a panel of non small cell lung cancer (NSCLC) cell lines, where Aurora B is highly expressed and rates of chromosome segregation are high, the experimental reduction of centromere-localized Aurora B levels, or the independent stabilization of kinetochore microtubule attachments, is sufficient to minimize genomic heterogeneity and limit

27 whole chromosome amplifications. We additionally find that suppression of nCIN limits acquired
28 drug resistance both *in vitro* and *in vivo*, and that sustained nCIN is rate limiting for tumor
29 relapse.
30

31 **Materials and Methods**

32 **Cell culture, protein expression and depletion**

33 PC9, H1299, A549, and HBEC3-KT (ATCC) cells were grown in RPMI1640 (Gibco, #61870036)
34 medium supplemented with 10% fetal bovine serum (Sigma, #16140071) and 1%
35 penicillin/streptomycin (Gibco, #15070063). All cells were cultured at 37°C and 5% CO2. High
36 resolution immunofluorescence imaging with DNA stain (DAPI) is used to monitor and confirm
37 cell lines are free of *Mycoplasma* contamination. For short term knock down of targets, 50nM
38 pool siRNAs (non-targeted pool or a pool of 4 siRNAs to Wapl; Dharmacon-ON-TARGETplus
39 Human Wapl siRNA-SMARTpool) were transfected using RNAiMax (ThermoFisher, #13778100)
40 transfection reagent according to the manufacturer's instruction, or alternatively infected with a
41 lentiviral construct containing a shRNA hairpin for constitutive (pLK0.1-Puro) or doxycycline
42 inducible (tet-pLK0-Puro) depletion. Stable hairpin-expressing clones were selected with
43 Puromycin for 7-10 days. Induced depletion was achieved by the addition of 2μg/ml doxycycline
44 for a minimum of 48 hours.
45

46 **Immunofluorescence and Fluorescence *in situ* hybridization**

47 Cultured cells or single cell suspensions derived from tumors were grown on coverslips, fixed,
48 and stained for Aurora B (BD Biosciences, #611082), ACA (Antibodies Inc, #15-234), tubulin
49 (Santa Cruz, #5286), CENPA S7p (Cell Signaling, #2187), and/or CENPA (Enzo Life Sciences,
50 ADI-KAM-CC006-E) as previously described [19, 20]. To assess kinetochore microtubule
51 stability cells were incubated in ice cold RPMI for 5 minutes (PC9 and A549) or 10 minutes

52 (H1299) prior to fixation and staining. Fluorescence *in situ* hybridization with centromeric probes
53 and quantification of numerical heterogeneity was performed as previously described in [21]
54 using alpha satellite-specific probes for chromosomes 2,6,7,8 and 10 (Cytocell, #LPE002R,
55 006G, 007G, 008R, 010R). For FISH from tumors, single cell suspensions were made by gently
56 grinding tumors between two glass slides and culturing with continued drug treatment for 3-5
57 days. Cells were then collected and processed as above. Clonal Numerical Heterogeneity (NH)
58 of a population was determined by scoring >300 cells per clone/tumor for copy number for
59 chromosome probe (assessed in pairs) to determine the modal copy number, and the fraction of
60 cells deviating from that number (i.e., the numerical heterogeneity). A given copy number with
61 greater than 20% prevalence in a population was considered to be a stable subclone and not
62 included in the numerical heterogeneity score. Data is represented for individual chromosomes,
63 or alternatively, as average NH across all chromosomes measured for a given sample. A
64 students' 2-tailed t-test was used to determine statistical significance.
65
66 ***In vivo* tumor growth and relapse assays**
67 Eight-week old male and female Crl:NU-*Foxn1*^{nu} mice (stock #088) were purchased from
68 Charles River Laboratory and maintained in a pathogen-free facility. All animal experiments
69 were performed in accordance with institutional regulations after protocol review and approval
70 by Worcester Polytechnic Institute's Institutional Animal Care and Use Committee.
71
72 For *in vivo* growth assays, three cohorts of 5 mice each were injected subcutaneously in the
73 flank with $5x10^6$ PC9 cells. 2 cohorts received PC9 cells expressing a tetracycline-inducible
74 shWapl expression construct. One of these two cohorts was administered 2 μg/ml doxycycline
75 in the drinking water. All three cohorts were monitored daily and tumor size measured 3x/week.
76 Mice were humanly sacrificed, and tumor tissue collected when tumor volume reached $300mm^3$.
77 For tumor relapse studies, tumor xenografts were generated as described above in 40 mice.

78 Xenograft tumor formation was observed in 38 mice. Once tumors reached a size of 300mm^3
79 mice were randomized equally into a minus or plus doxycycline group. All mice were given
80 50mg/kg Gefitinib (Selleckchem, #ZD1839) by oral gavage following a 5 day on and 2 day off
81 cycle. Mice were monitored daily and tumor size measured 3x/week to monitor tumor regression
82 and relapse. Once relapsed tumors reached a size of 300mm^3 mice were humanly sacrificed,
83 tumors harvested and frozen or cultured for subsequent experimental analysis.
84 Please see supplemental material for extended methods.
85
86 **Data Availability**
87 The data generated in this study are available within the article and its supplementary data files.
88
89 **Results**
90 **Chromosome segregation errors in NSCLC cells correspond with high expression and**
91 **enhanced mitotic centromere localization of Aurora B**
92 Non small lung cancer (NSCLC) cells frequently exhibit high levels of whole chromosome
93 instability (nCIN), a feature that has been experimentally linked to acquired drug resistance [1,
94 3-6, 22]. To understand the molecular changes that correspond with segregation errors and
95 nCIN in NSCLC cells we first identified a panel of NSCLC cell lines that exhibit mitotic defects
96 and chromosome copy number heterogeneity consistent with nCIN (A549, H1299, and PC9;
97 [21]). Using immunofluorescence microscopy to assess chromosome segregation we confirm
98 that NSCLC lines A549, H1299, and PC9 all exhibit high rates of lagging chromosomes during
99 anaphase that are indicative of mitotic chromosome segregation errors (Figure 1A). Frequent
100 high rates of whole chromosome segregation errors during mitosis contribute to genomic
101 heterogeneity within a cell population that can be assessed using FISH-based approaches to
102 measure population-level numerical heterogeneity (NH) for individual chromosomes. Using
103 centromeric probes for chromosomes 6, 7, 8, and 10 we find that, consistent with frequent

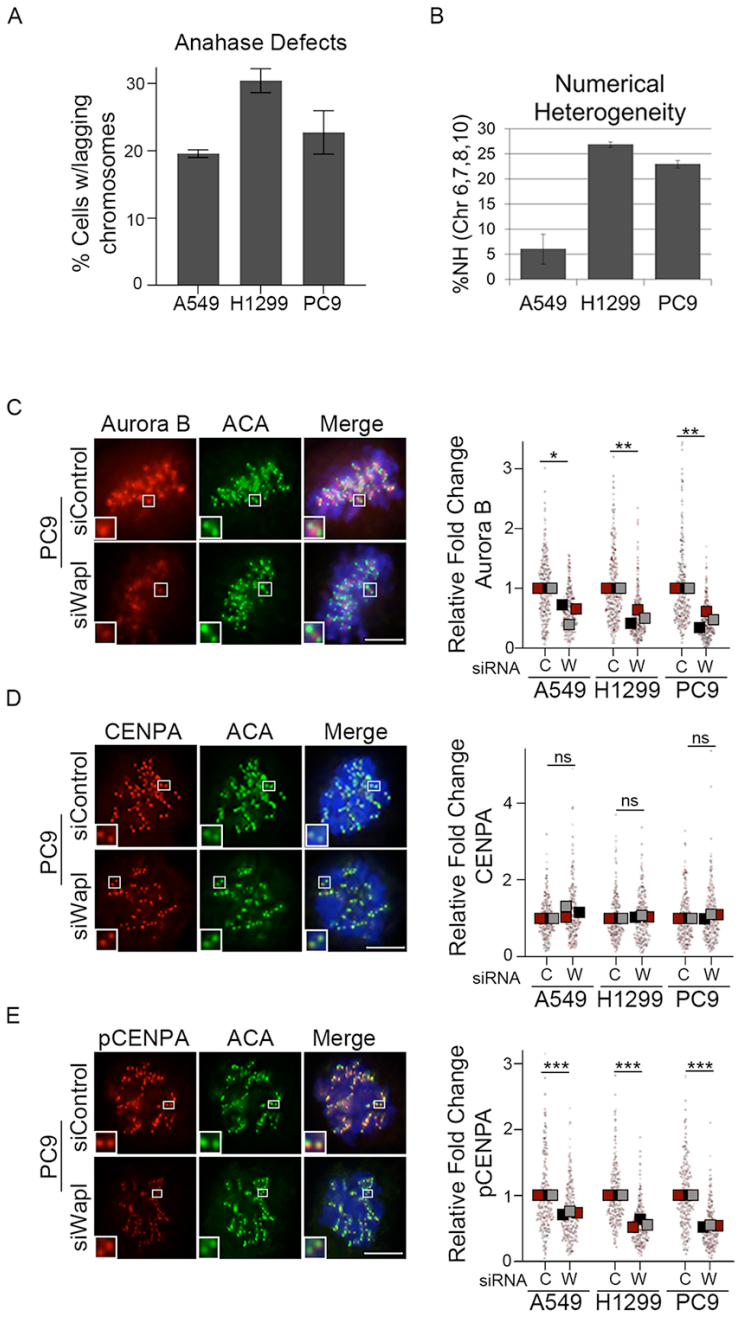

Figure 1: Enrichment of cohesion in NSCLC cells decreases Aurora B localization and activity at the centromere A) Quantification of anaphase lagging chromosomes in NSCLC cell lines B) NSCLC cell populations labelled with centromere enumeration FISH probes for chromosomes 6, 7, 8, and 10 and quantified for numerical heterogeneity. A minimum of 300 cells for each chromosome probe were scored and averaged per cell line. C-E) Representation and quantification of centromere localized Aurora B, CENPA (total) and pCENPA (pSer7) in PC9 cells treated with non-targeting (siControl) or Wapl specific (siWapl) siRNA. A minimum of 90 kinetochore pairs were measured (3/cell for 30 cells), for each of 3 biological replicates. Insets are of individual kinetochore pairs at 4x magnification. Scale bars are 5μm. Here and throughout *: p< 0.05, **: p<0.01; ***: p<0.001.

mitotic errors, populations of A549, H1299 and PC9 cells exhibit NH scores ranging from ~7-25% (Figure 1B).

106 Aurora B kinase, an important regulator of mitotic chromosome segregation and the mitotic
107 spindle assembly checkpoint, is commonly overexpressed in non small cell lung cancer, where
108 nCIN is also prevalent [23-25]. Consistent with these earlier studies, we find that Aurora B
109 kinase is highly expressed in our panel of NSCLC cells, when compared to the normal lung
110 epithelial cell line HBEC3-KT (Supplemental Figure 1A). Aurora B regulation of mitotic
111 chromosome segregation is largely dependent on its localization at centromeres where it
112 phosphorylates key substrates that regulate the stability of kinetochore-microtubule attachments
113 [26-30] Importantly, we find that centromere localization of Aurora B in our panel of NSCLC cell
114 lines mirrors overall expression levels of this kinase such that Aurora B localization at
115 centromeres is increased, on average, two to five-fold over that seen in HBEC3-KT cells
116 (Supplemental Figure 1B).
117
118 **Centromere localization and activity of Aurora B in NSCLC is sensitive to cohesion**
119 Aurora B localization is sensitive to changes in cohesin regulation such that redistribution of the
120 cohesin complex from pericentromere enrichment to distribution along chromosome arms leads
121 to a concurrent redistribution of Aurora B along chromosome arms and a reduction in its
122 centromere localization [19, 31-33] Therefore, to test the impact of high centromere Aurora B
123 levels in the mitotic defects observed in these NSCLC lines without altering overall Aurora B
124 protein levels, we first experimentally manipulated the distribution of the cohesin complex.
125 Enhancement of chromosome cohesion along chromosome arms was achieved using si- and
126 sh-RNA approaches to deplete Wapl, a well-characterized negative regulator of the cohesin
127 complex [34] (Supplemental Figure 2A & B). Wapl associates with the cohesin complex to
128 regulate its dynamic association with chromatin throughout the cell cycle [35] such that Wapl
129 depletion blocks cohesin complex dissociation from chromosomes during early mitosis. We
130 used immunofluorescence imaging of metaphase cells to identify and measure inter-kinetochore
131 distances as a readout of functional centromere cohesion. This demonstrated that Wapl

132 knockdown enhanced cohesion, as evidenced by a reduction in interkinetochore distance
133 (Supplemental Figure 2C).
134
135 Using quantitative immunofluorescence, we find that depletion of Wapl perturbs Aurora B
136 localization such that centromere-localized Aurora B levels in all three NSCLC lines is reduced
137 by ~50% when Wapl is depleted (Figure 1C and Supplemental Figure 3A). Western blot
138 analysis of mitotic cells indicate that this change in Aurora B localization does not arise due to
139 Wapl-dependent changes in Aurora B expression (Supplemental Figure 2B). Consistent with
140 reduced centromere localization and activity of Aurora B, we see comparable reduction in the
141 phosphorylation, but not localization, of key Aurora B substrate CENPA (Total and CENPA pS7:
142 Figure 1D & E, Supplemental Figure 3B & C).
143
144 **Modulation of Aurora B activity suppresses kinetochore-microtubule dynamics and**
145 **chromosome segregation errors**
146 Aurora B kinase is a master regulator of microtubule dynamics such that Aurora B localization
147 and kinase activity promotes the dynamic turnover of kinetochore microtubule attachments. The
148 fidelity of chromosome segregation has been shown to be sensitive to both increased and
149 decreased Aurora B activity, and hence corresponding decreased and increased stability of
150 kinetochore-microtubule attachments [8, 16, 17, 36, 37]. Consistent with this activity, we find
151 that kinetochore fibers in Wapl-depleted cells, where Aurora B localization at centromeres had
152 been reduced, exhibit decreased sensitivity to cold-induced microtubule depolymerization
153 compared to control cells (Figure 2A). This suggests kinetochore microtubule attachments are
154 stabilized by the redistribution of Aurora B away from the centromere that occurs following Wapl
155 depletion. We next assessed mitotic fidelity in these cells and find that enhancement of
156 chromosome arm cohesion, via Wapl depletion, is sufficient to reduce the incidence of lagging
157 chromosomes during anaphase in both H1299 and PC9 cells (Figure 2C). Similarly, partial

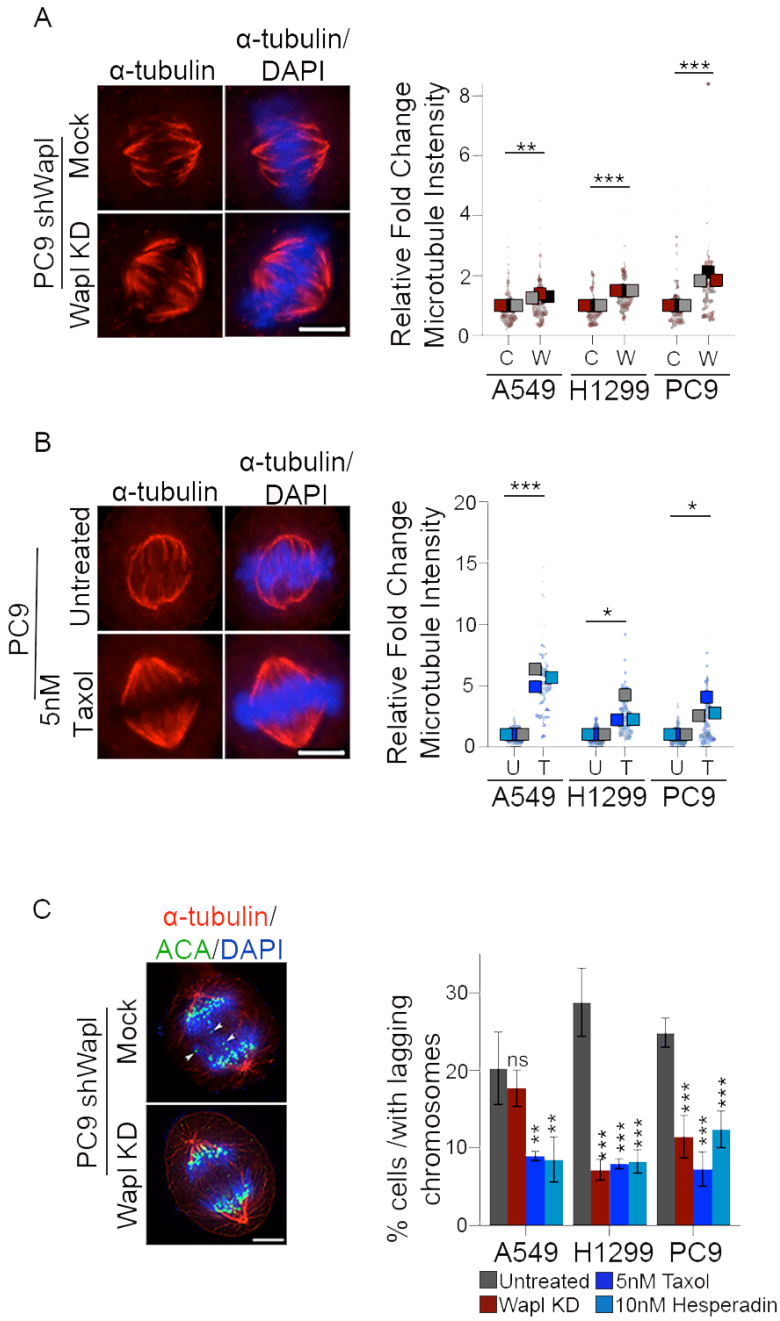

Figure 2: Anaphase segregation errors in NSCLC cells are reduced by microtubule stabilizing perturbations A & B) Representation and quantification of cold stable microtubules in PC9 cells depleted of Wapl (A) or treated with 5nM Taxol (B). C) Representation and quantification of anaphase lagging chromosomes in NSCLC cells following Wapl depletion, or treatment with 5nM Taxol, or 10nM Hesperdain. White arrow heads indicate individual lagging chromosomes. A minimum of 30 metaphase or anaphase cells were scored per population for each of 3 biological replicates. Scale bars are 5μm.

158 inhibition of Aurora B activity with the small molecule inhibitor Hesperdain, is sufficient to

159 suppress mitotic defects in all three NSCLC lines (Figure 2C).

160 To directly test the role of microtubule dynamics in the high frequency of mitotic errors observed
161 in this panel of NSCLC cells, we treated cells with a microtubule-stabilizing concentration of
162 Taxol prior to assessing mitotic fidelity. We find that following acute treatment (1h) with 5nM
163 Taxol, or long-term treatment (6 weeks) with 1nM Taxol, cells exhibit both resistance to cold-
164 induced microtubule depolymerization and reduction in anaphase lagging chromosomes,
165 comparable to that seen following Wapl depletion (Figure 2B & C, Supplemental Figure 4A & B).
166
167 To next assess if enhanced cohesion and reduction of anaphase defects is sufficient to
168 suppress nCIN, PC9 cells were engineered to constitutively express one of two different shRNA
169 hairpin constructs designed to target Wapl mRNA for depletion. Single cell clones were derived
170 from parental and Wapl-deficient PC9 cells and analyzed for numerical heterogeneity (NH).
171 Individual clones derived from PC9 cells expressing an empty PLK0.1 vector exhibit NH values
172 of 18-31% for chromosome 6, and up to 20-40% for chromosome 2. NH for both chromosomes
173 was reduced ~2-3-fold in Wapl-deficient PC9 cell clones (chromosome 6: 3-12%, chromosome
174 2: 5-24%) (Supplemental Figure 2D), indicating that enhanced cohesion is sufficient to suppress
175 nCIN. Together, these data support a model whereby increased Aurora B activity and/or highly
176 dynamic kinetochore microtubule attachments underlie nCIN in NSCLC cells.
177
178 **Suppression of CIN limits drug tolerance in NSCLC cells.**
179 Activating mutations within the EGFR gene that drive tumor cell proliferation are present in
180 nearly a quarter of all NSCLCs [38]. Patients with such mutations are commonly treated with
181 EGFR tyrosine kinase inhibitors (TKIs) [39]. However, the majority of patients treated with
182 EGFR TKIs ultimately develop resistance with nearly 60% of resistant or relapsed tumors
183 exhibiting resistance-conferring mutations in the EGFR gene, making this the most frequent
184 mechanism of EGFR TKI resistance [40]. PC9 cells exhibit an activating deletion in exon 19 of
185 EGFR that drives cell proliferation and renders them sensitive to EGFR TKIs [41]. Like tumors in

186 patients, these cells commonly acquire resistance to EGFR TKIs via acquisition of a secondary
187 Threonine to Methionine mutation in EGFR (T790M) [40]. While nCIN in NSCLC, and other
188 cancer contexts, has been correlated with acquired drug resistance [5, 23, 42], the impact of
189 nCIN on mutation-based mechanisms of acquired drug resistance remain unclear.
190 Drug response is sensitive to cell proliferation rates and the impact of aneuploidies that result
191 from nCIN have alternatively been demonstrated to promote tumor cell growth or to reduce
192 proliferative capabilities [43, 44]. Therefore, we first assessed proliferative capacity of PC9 cells
193 with and without constitutive nCIN/Wapl depletion (Mock and Wapl KD, respectively) or
194 following acclimation to microtubule-stabilizing concentrations of Taxol. Importantly, in all clones
195 tested, proliferation rates with or without Wapl depletion or Taxol treatment, when grown in the
196 absence of TKI treatment, were comparable (Supplemental Figure 4C-E). Similarly, anchorage
197 independent colony formation assays of growth in soft agar revealed similar colony number and
198 size, irrespective of Wapl/nCIN status (Supplemental Figure 4F), indicating that suppression of
199 nCIN alone does not alter drug naïve PC9 cell growth.
200
201 Next we assessed the response of cells, with and without Wapl depletion or Taxol treatment, to
202 the EGFR TKI Gefitinib. EGFR activity results in phosphorylation of EGFR and downstream
203 targets (such as ERK) and promotes cell proliferation. Western blot analyses indicate that PC9
204 cells with either mock or induced Wapl depletion or treated with 1nM Taxol are initially similarly
205 responsive to Gefitinib: all populations show dramatic reduction of EGFR-dependent
206 phosphorylation (phospho EGFR: Tyr1068 & phospho ERK: Tyr 202/Tyr 204) (Figure 3A).
207 Nevertheless, following 4 weeks of continuous treatment with a sub-lethal dose of Gefitinib
208 drug-tolerant cells slowly form colonies that can be detected with crystal violet stain. Following
209 long-term exposure to Gefitinib, Wapl-depleted and Taxol-treated PC9 cells exhibit a dramatic
210 reduction in the number and size of drug tolerant colonies that arise while under Gefitinib
211 treatment (Figure 3B & C).

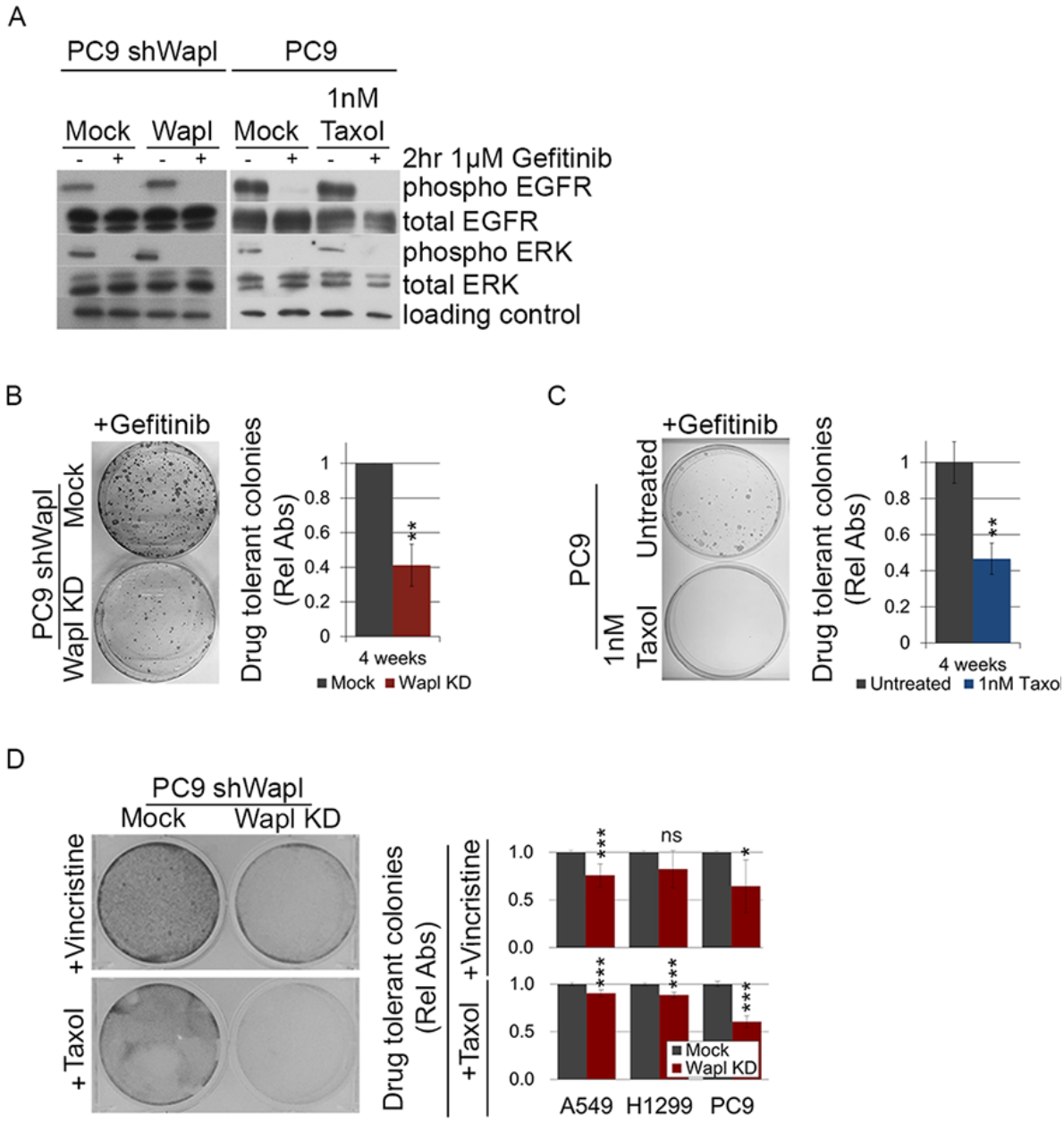

Figure 3: Suppression of nCIN limits drug tolerance A) Total and phosphorylated levels of EGFR and ERK in PC9 cells with induced depletion of Wapl or 1nM Taxol treatment following Gefitinib treatment. B & C) Crystal Violet staining and quantification of drug tolerant colonies of control and Wapl depleted PC9 cells following extended culture of Wapl depleted (B) or Taxol treated (C) cells in presence of 1mM Gefitinib D) Crystal Violet staining and quantification of drug tolerant colonies of control and Wapl depleted NSCLC cells following extended culture in the presence of Vincristine or Taxol. Representative images and quantification reflect data from three independent biological replicates.

212

213 Acquired resistance to other clinically relevant therapeutics such as Vincristine and Paclitaxel

214 have been reported in NSCLC [45-50]. Therefore, to next test whether the impact of

215 suppression of CIN on drug tolerance is specific to Gefitinib or instead may similarly limit the
216 outgrowth of cells tolerant to other therapeutic agents, we performed *in vitro* drug tolerance
217 assays in A549, H1299, and PC9 cells with and without constitutive depletion of Wapl in the
218 presence of either Vincristine or Paclitaxel. Over the course of 14 weeks the concentration of
219 these drugs was doubled every 4 days until drug tolerant cells emerged. Comparative measures
220 of cell numbers in each condition were approximated using crystal violet staining. Following
221 long-term treatment with either Vincristine or Paclitaxel, all three NSCLC lines constitutively
222 depleted of Wapl show reduction in the number of drug-tolerant cells (Figure 3D). Importantly,
223 cells constitutively depleted of Wapl for the duration of the drug sensitivity assay show no
224 change in proliferation rates, suggesting decreased tolerance to Vincristine or Paclitaxel cannot
225 be accounted for by changes in proliferation rate following Wapl depletion (Supplemental Figure
226 4E). These data suggest that nCIN permits acquisition of drug tolerance to promote continued
227 proliferation.
228
229 **Chromosome Instability informs mechanism of TKI drug resistance.**
230 To better understand the relationship between nCIN-dependent genomic changes that may
231 promote or permit resistance to drug therapy we characterized four drug-tolerant clones from
232 each of the parental and Wapl-depleted populations that were exposed to long-term Gefitinib
233 treatment. Clones were selected and expanded under culture conditions that maintained 1μM
234 Gefitinib and mock or induced Wapl depletion, as appropriate. Importantly, in both Wapl-
235 depleted and Wapl-proficient contexts, drug tolerant PC9 cells that persist following long term
236 exposure to Gefitinib continue to exhibit features consistent with Wapl status: single colonies
237 derived from Mock-depleted cells have frequent anaphase defects and a high measure of NH
238 and whole chromosome amplifications while Wapl-depleted cells have reduced anaphase
239 defects and less numerical heterogeneity (Figure 4A-C).
240

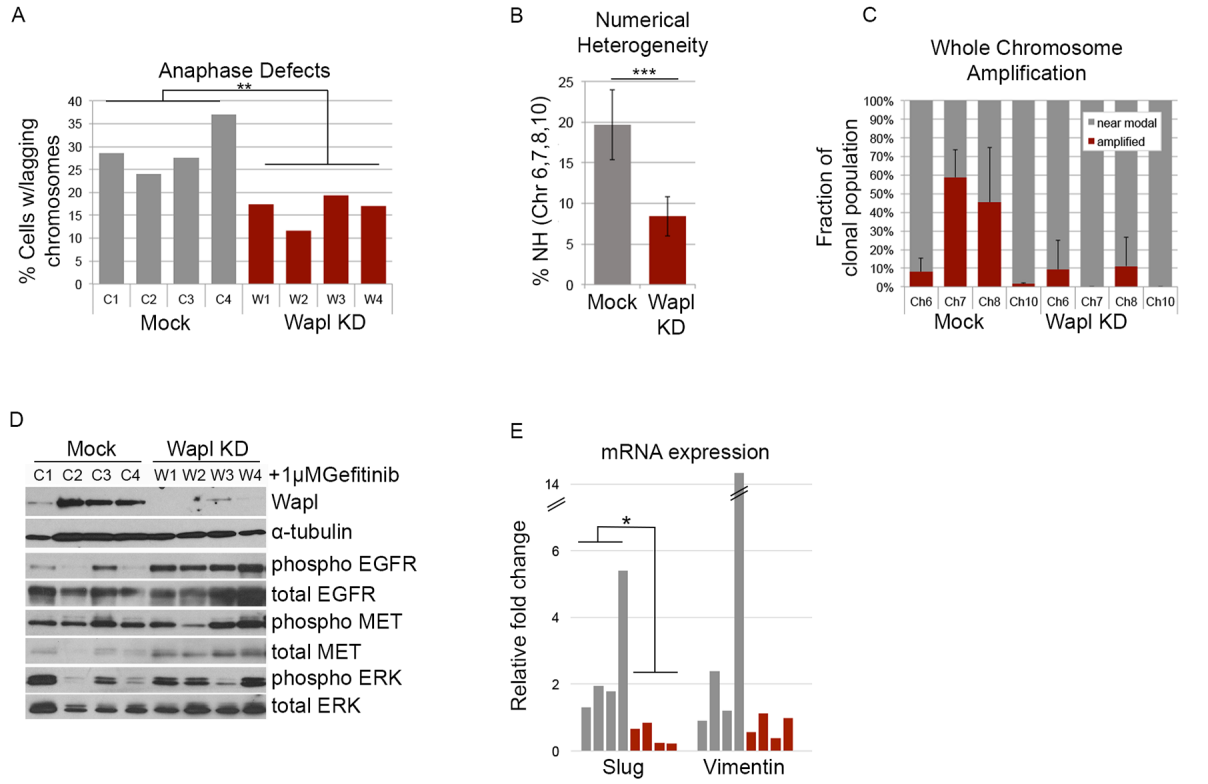

Figure 4: Suppression of nCIN influences mechanisms of drug tolerance in PC9 cells. A) Quantification of anaphase cells exhibiting lagging chromosomes in clonal populations of Gefitinib-tolerant cells with (Wapl KD) or without (Mock) induced Wapl depletion. B & C) Gefitinib-tolerant PC9 clonal populations derived with or without Wapl depletion labelled with centromere enumeration FISH probes for chromosomes 6, 7, 8, and 10 and quantified for chromosome copy number. Represented as average numerical copy number across all chromosomes assessed (B) and fraction of cells with modal or amplified copies of the indicated chromosomes (C). A minimum of 300 cells per condition per centromere probe assessed were scored. D) Western blot showing Wapl levels and EGFR pathway status in four each of mock and Wapl-depleted Gefitinib-tolerant clones. E) qPCR analysis of mRNA levels indicative of EMT pathway activation (Slug, Vimentin) in Mock and Wapl-depleted Gefitinib-tolerant clones.

241 Cells that acquire tolerance or resistance to TKI activity do so by restoring or bypassing EGFR
242 kinase function to activate downstream pathway components and promote proliferation [40].
243 Although the emergence of drug tolerant clones is decreased significantly by Wapl depletion,
244 molecular characterization of EGFR pathway function indicates that drug tolerant clones that do
245 arise from both Mock- and Wapl-depleted populations similarly exhibit phosphorylation of ERK,
246 a downstream target in the EGFR pathway (Figure 4D). In contrast, Wapl-depleted PC9 clones,
247 but not Mock-depleted PC9 clones, exhibit EGFR auto phosphorylation (Figure 4D). This
248 phosphorylation is dependent on EGFR kinase activity and suggests drug-tolerant clones that
249 lack nCIN (Wapl KD) primarily arise through the acquisition of resistance-conferring mutations

250 that impair TKI binding, while clones that sustain nCIN (Mock) likely exploit other mechanisms of
251 drug tolerance [38-40, 47].
252
253 Alternative pathways reported to promote TKI resistance in NSCLC include amplification of
254 EGFR, amplification of the receptor tyrosine kinase MET [47], and/or activation of epithelial to
255 mesenchymal transition (EMT) [51-53]. To understand if these alternative pathways could
256 explain tolerance of Mock- depleted PC9 clones to Gefitinib treatment, we first assessed copy
257 number of chromosome 7, on which both EGFR and MET genes are located. Drug naïve PC9
258 cells have a modal copy number of four for chromosome 7, as do drug tolerant Wapl-depleted
259 clones. In contrast, nearly 60% of drug tolerant Mock-depleted cells have >8 copies of
260 chromosome 7 (Figure 4C, Supplemental Figure 5). We next looked at expression of key EMT
261 transcription factor SLUG and found it to be upregulated 2-fold in 3 out of 4 Mock-depleted
262 clones, but not in any of the Wapl-depleted clones (Figure 4E). The gene that encodes for
263 SLUG, SNAI2, is located on chromosome 8p, adjacent to the centromere. In support of a model
264 whereby CIN influences the mechanism of TKI resistance, single cell analysis of chromosome 8
265 copy number indicates that the same 3 Mock-depleted clones with increased SLUG expression
266 also exhibit amplification of chromosome 8 (Figure 4C, Supplemental Figure 5). Consistent with
267 SNAI2 amplification and increased Slug expression, Vimentin, a widely used marker of EMT
268 and a Slug target gene is also increased 2 to 12-fold in Mock-depleted clones (Figure 4E).
269 Together these data suggest that nCIN influences the mechanism of acquired drug resistance.
270 Without nCIN, mutation-driven mechanisms of drug resistance dominate, but the acquisition of
271 such mutations are slow, particularly in drug treated populations with limited proliferation, and as
272 a result drug resistant colonies are slow to emerge. Through whole chromosome gains and
273 losses hundreds to thousands of genes may become mis-regulated in a single cell division. In
274 this way nCIN has the capacity to promote cellular changes that contribute to drug tolerance.
275

276 **Wapl depletion is sufficient to suppress nCIN *in vivo***

277 To assess how cohesion-dependent suppression of nCIN impacts tumor initiation and growth *in*
278 *vivo*, PC9 cells with or without a tetracycline-inducible shWapl construct were injected
279 subcutaneously into the flanks of nude mice to generate 3 cohorts: one with parental PC9 cells,
280 and two with PC9 cells that harbor the inducible shWapl construct (Supplemental Figure 6A).
281 One cohort of PC9 shWapl mice received doxycycline in the drinking water to induce expression
282 of the Wapl-targeting hairpin throughout the duration of tumor initiation and growth. The cohort
283 injected with the PC9 parental cell line similarly received doxycycline in the water as a negative
284 control. Tumor initiation was comparable in all three cohorts of mice, as was rate of tumor
285 growth (Supplemental Figure 6B, Supplemental Figure 7A). To confirm the efficiency of Wapl
286 depletion and the suppression of nCIN in response to doxycycline treatment *in vivo*, tumors from
287 mice in each cohort were excised when they reached 300cm^3 and subjected to analysis.
288 Quantitative PCR analyses confirm that depletion of Wapl mRNA and protein levels were
289 achieved and sustained during tumor initiation in response to doxycycline (Supplemental Figure
290 6C). Consistent with *in vitro* assays, cells derived from Wapl-deficient tumors exhibit fewer
291 anaphase defects (Supplemental Figure 6D) and less intra-tumor chromosome numerical
292 heterogeneity (Supplemental Figure 6E). Together these data indicate that suppression of nCIN
293 in NSCLC cells is not in itself sufficient to limit tumor initiation and growth *in vivo*.

294

295 **nCIN is a driver of drug resistance *in vivo***

296 To test the role of nCIN in tumor relapse, the xenograft model described above was used to
297 establish mice that harbored inducible PC9 shWapl tumors. Once tumors reached a volume of
298 300mm^3, mice were put on a 5 days on, 2 days off (5+2) regimen of 50 mg/kg Gefitinib
299 treatment and randomly assigned to two cohorts. One cohort received doxycycline in the
300 drinking water to induce Wapl depletion concurrent with Gefitinib treatment, the other did not
301 (Figure 5A). Both cohorts of mice exhibited similar initial response to Gefitinib, with all tumors

302 exhibiting >50% recession within 2 weeks. In the 100 days following initial tumor recession mice

303 were sustained on a 5+2 drug regimen. During this time 37% (7/19) of Mock-depleted tumors

304 and 21% (4/19) of Wapl depleted tumors relapsed. Relapse of Wapl depleted tumors was

305 delayed by nearly 3 weeks compared to those without induced Wapl depletion (66 days vs 46

306 days for Mock depleted tumors) (Figure 5B, Supplemental Figure 7B). A similar frequency of the

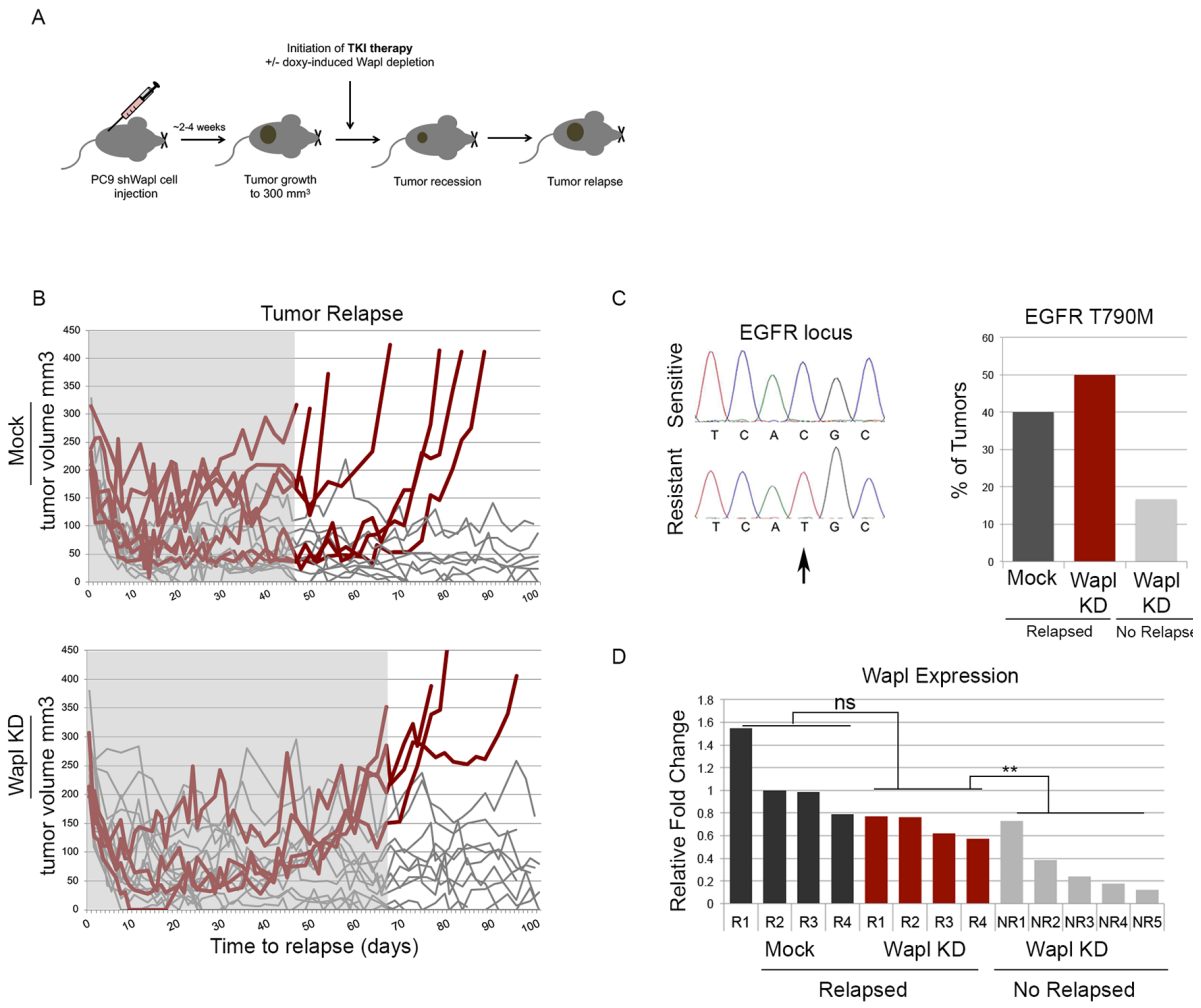

Figure 5: nCIN is a driving force for acquired drug resistance. A) Diagram of experimental set up: PC9 cells carrying an inducible shWapl construct were injected into the flank of the mice. Once tumors reached 300mm^3 mice were split into two cohorts: one was administered doxycycline in drinking water to induce Wapl depletion concurrent with Gefitinib via oral gavage, the other received Gefitinib alone. All mice were monitored for initial tumor recession and relapse. B) Time to relapse of tumors with uninduced (n=19) and induced Wapl depletion (n= 19). Red lines indicate tumors that relapsed in this time frame, gray lines indicate those that remained responsive to treatment. Shaded box indicates the minimum relapse free response to Gefitinib in each cohort. C) Visualization and quantification of C → T mutation that results in the T790M mutation in EGFR that confers resistance to TKI in tumors from each cohort. D) qPCR analysis of Wapl levels in control (Mock) and induced Wapl depletion (Wapl KD) that relapsed or not following Gefitinib treatment.

307 TKI resistance-conferring EGFR T790M mutation was detected in relapsed tumors from both
308 cohorts (Figure 5C). Interestingly, anaphase defects were similarly prevalent in all relapsed
309 tumors, regardless of cohort, indicating a selective pressure to maintain CIN during acquisition
310 of drug resistance (Supplemental Figure 7C). Consistent with this, all residual/non-relapsed
311 tumors analyzed from the Wapl depleted cohort sustained Wapl depletion while tumors that
312 relapsed expressed Wapl at levels comparable to the Mock-depleted cohort (Figure 5D). These
313 data support a model whereby re-establishment of Wapl expression/nCIN, or expansion of
314 clones that fail to silence Wapl/sustain nCIN, is limiting for acquired drug resistance and tumor
315 relapse (Figure 6).

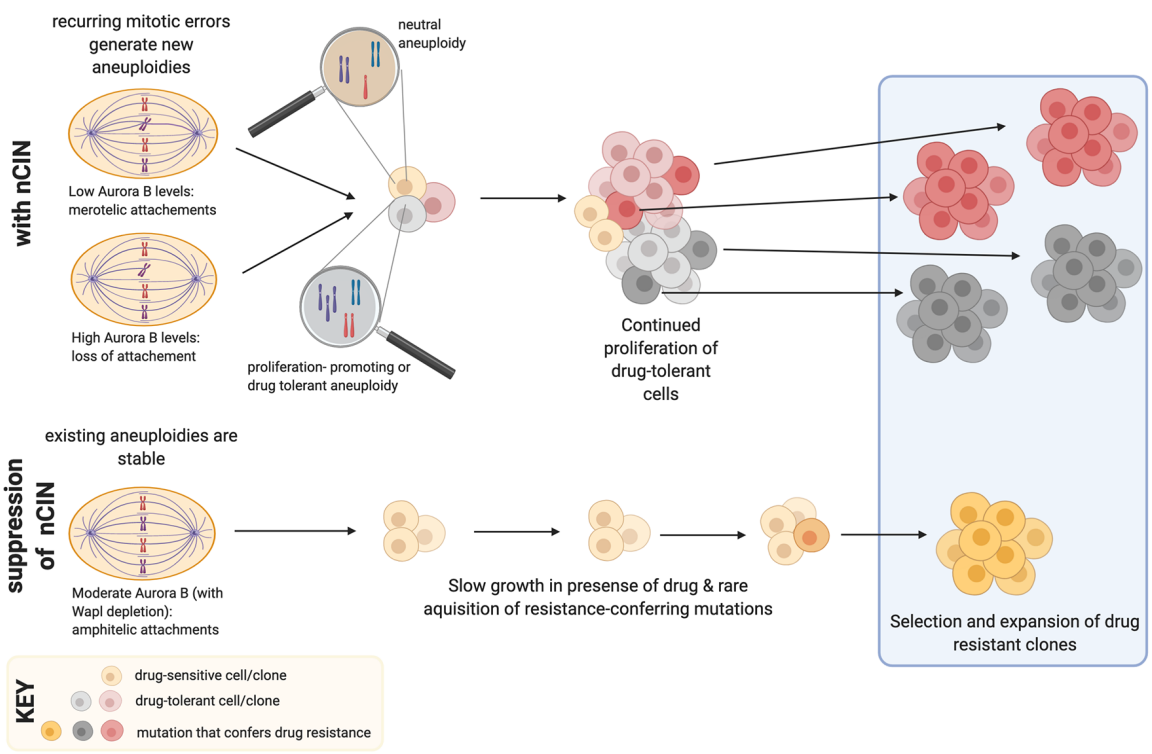

Figure 6: Mitotic defects that promote CIN enable generation of drug tolerant aneuploidies that permit continued growth and increased incidence of acquired drug resistance.

316

317 **Discussion**

318 Clonal mutations that enable resistance to targeted or chemotherapeutic approaches pose a
319 clinical challenge and remain a major cause of death in many cancer types [54]. Clinically and

320 experimentally, the degree of intra-tumor genomic heterogeneity, and underlying defects in
321 mitotic cell division have been functionally linked to tumor evolution, drug resistance, and
322 metastasis [3, 4, 6, 7, 55, 56]. In the context of NSCLC, identification of driver mutations in
323 EGFR and the initial clinical success of TKI treatment has been hampered by rapid and
324 prevalent acquisition of drug resistance [38]. Here, we present mechanistic evidence that nCIN
325 may arise from mis-regulation of cohesin-sensitive Aurora B kinase activity at centromeres and
326 deregulation of spindle microtubule dynamics. We propose that subsequent chromosome
327 amplifications contribute to a high incidence of acquired resistance to therapy. The reduction in
328 emergence of drug tolerant clones following experimental suppression of nCIN demonstrate that
329 whole chromosome copy number changes create a favorable environment for continued
330 proliferation while resistance-conferring mutations are attained. Consistent with this, we find that
331 a selective pressure exists *in vivo* to maintain or re-establish nCIN to facilitate robust acquisition
332 of drug resistance and tumor relapse (Figures 5 &6).
333
334 **Whole chromosome segregation errors enable tumor evolution and drug resistance**
335 Our analysis examined isogenic PC9 cells that primarily differ, at least initially, in their nCIN
336 status. Our results indicate that nCIN contributes to drug resistance by allowing for the
337 generation of whole chromosome amplifications that harbor key drug tolerance genes (like
338 EGFR, MET, and SNAI2/SLUG) and promote continued proliferation in the presence of TKI. In
339 the absence of an increased mutation rate, this continued proliferation is key to enable the
340 acquisition of replication-dependent mutations that confer robust drug resistance and tumor
341 relapse. Such adaptive mutability may be particularly relevant to the mis-segregation and
342 subsequent selection for amplification of chromosome 7, which contains both MET and EGFR
343 genes. Increased EGFR gene copy number both promotes proliferation [40] and, by virtue of
344 having more EGFR gene templates for replication-acquired mutation, increases the apparent
345 mutability of individual cells [57]. These findings are consistent with previous studies showing

346 selective pressure for cancer cells to sustain nCIN and demonstrating that high levels of nCIN
347 can drive the generation and selection of drug-resistant clones [6, 7, 58, 59].
348
349 **High mutation rates may preclude the need for nCIN in acquired drug resistance.**
350 In the absence of nCIN, resistance is limited to the clonal amplification of cells with pre-existing
351 amplifications or mutations, and those that acquire chromosome amplifications through rare
352 segregation errors. An increase in mutation rate may negate the need for nCIN by increasing
353 the frequency at which resistance-conferring mutations are generated in each cell cycle.
354 Consistent with this view, high mutation rates and nCIN have been found to be mutually
355 exclusive in various cancer contexts [60].
356
357 **nCIN as a therapeutic target**
358 Similar to what we demonstrate here, work from other groups has shown that presence of nCIN
359 can promote acquisition of drug resistance and is a mechanism to evade oncogene addiction [5,
360 58]. Our data additionally show that suppression of segregation errors in a cancer context is
361 achievable and that reduction of nCIN can limit mechanisms of acquired drug resistance.
362 Indeed, due to its role in regulation of chromosome segregation, Aurora B is a provocative drug
363 target, and its inhibition has recently been shown to be efficacious in limiting proliferation of TKI-
364 resistant NSCLC cells [61]. Together these data propose that pathways that promote nCIN may
365 serve as valuable drug targets, alone, or as co-therapies to enhance or prolong response to
366 targeted therapeutic approaches.
367
368 **Acknowledgements**
369 This work was supported by a Smith Family Award for Excellence in Biomedical Research and
370 R00CA182731 to ALM.
371

372 **Author Contributions**

373 ALM conceived and devised the study. ALM, EAC, and NMH designed the experiments. ALM,
374 NMH, EAC, and CPH performed the experiments. ALM wrote the manuscript with input and
375 approval from all authors.

376

377 **Declaration of Interests**

378 Authors declare no competing interests

References

1 Baker DJ, Jin F, Jeganathan KB, van Deursen JM. Whole chromosome instability caused by Bub1 insufficiency drives tumorigenesis through tumor suppressor gene loss of heterozygosity. *Cancer Cell* 2009; 16: 475-486.

2 Weaver BA, Silk AD, Montagna C, Verdier-Pinard P, Cleveland DW. Aneuploidy acts both oncogenically and as a tumor suppressor. *Cancer Cell* 2007; 11: 25-36.

3 Choi CM, Seo KW, Jang SJ, Oh YM, Shim TS, Kim WS *et al*. Chromosomal instability is a risk factor for poor prognosis of adenocarcinoma of the lung: Fluorescence in situ hybridization analysis of paraffin-embedded tissue from Korean patients. *Lung Cancer* 2009; 64: 66-70.

4 McClelland SE, Burrell RA, Swanton C. Chromosomal instability: a composite phenotype that influences sensitivity to chemotherapy. *Cell Cycle* 2009; 8: 3262-3266.

5 Sotillo R, Schvartzman JM, Socci ND, Benezra R. Mad2-induced chromosome instability leads to lung tumour relapse after oncogene withdrawal. *Nature* 2010; 464: 436-440.

6 Lukow DA, Sausville EL, Suri P, Chunduri NK, Wieland A, Leu J *et al*. Chromosomal instability accelerates the evolution of resistance to anti-cancer therapies. *Dev Cell* 2021; 56: 2427-2439 e2424.

7 Ippolito MR, Martis V, Martin S, Tijhuis AE, Hong C, Wardenaar R *et al*. Gene copy-number changes and chromosomal instability induced by aneuploidy confer resistance to chemotherapy. *Dev Cell* 2021; 56: 2440-2454 e2446.

8 Bakhoum SF, Genovese G, Compton DA. Deviant kinetochore microtubule dynamics underlie chromosomal instability. *Curr Biol* 2009; 19: 1937-1942.

9 Godek KM, Kabeche L, Compton DA. Regulation of kinetochore-microtubule attachments through homeostatic control during mitosis. *Nat Rev Mol Cell Biol* 2015; 16: 57-64.

10 Taylor AM, Shih J, Ha G, Gao GF, Zhang X, Berger AC *et al*. Genomic and Functional Approaches to Understanding Cancer Aneuploidy. *Cancer Cell* 2018; 33: 676-689.e673.

11 Nagy Á, Lánczky A, Menyhárt O, Győrffy B. Validation of miRNA prognostic power in hepatocellular carcinoma using expression data of independent datasets. *Sci Rep* 2018; 8: 9227.

12 Hindriksen S, Lens SMA, Hadders MA. The Ins and Outs of Aurora B Inner Centromere Localization. *Front Cell Dev Biol* 2017; 5: 112.

13 González-Loyola A, Fernández-Miranda G, Trakala M, Partida D, Samejima K, Ogawa H *et al*. Aurora B Overexpression Causes Aneuploidy and p21Cip1 Repression during Tumor Development. *Mol Cell Biol* 2015; 35: 3566-3578.

14 Abe Y, Sako K, Takagaki K, Hirayama Y, Uchida KS, Herman JA *et al*. HP1-Assisted Aurora B Kinase Activity Prevents Chromosome Segregation Errors. *Dev Cell* 2016; 36: 487-497.

15 Broad AJ, DeLuca KF, DeLuca JG. Aurora B kinase is recruited to multiple discrete kinetochore and centromere regions in human cells. *J Cell Biol* 2020; 219.

16 Hauf S, Cole RW, LaTerra S, Zimmer C, Schnapp G, Walter R *et al*. The small molecule Hesperadin reveals a role for Aurora B in correcting kinetochore-microtubule attachment and in maintaining the spindle assembly checkpoint. *J Cell Biol* 2003; 161: 281-294.

17 Muñoz-Barrera M, Monje-Casas F. Increased Aurora B activity causes continuous disruption of kinetochore-microtubule attachments and spindle instability. *Proc Natl Acad Sci U S A* 2014; 111: E3996-4005.

18 Huang H, Lampson M, Efimov A, Yen TJ. Chromosome instability in tumor cells due to defects in Aurora B mediated error correction at kinetochores. *Cell Cycle* 2018; 17: 2622-2636.

19 Kleyman M, Kabeche L, Compton DA. STAG2 promotes error correction in mitosis by regulating kinetochore-microtubule attachments. *J Cell Sci* 2014; 127: 4225-4233.

20 Herlihy CP, Hahn S, Hermance NM, Crowley EA, Manning AL. Suv420 enrichment at the centromere limits Aurora B localization and function. *J Cell Sci* 2021; 134.

21 Manning AL, Benes C, Dyson NJ. Whole chromosome instability resulting from the synergistic effects of pRB and p53 inactivation. *Oncogene* 2014; 33: 2487-2494.

22 Swanton C, Nicke B, Schuett M, Eklund AC, Ng C, Li Q *et al*. Chromosomal instability determines taxane response. *Proc Natl Acad Sci U S A* 2009; 106: 8671-8676.

23 Yu J, Zhou J, Xu F, Bai W, Zhang W. High expression of Aurora-B is correlated with poor prognosis and drug resistance in non-small cell lung cancer. *Int J Biol Markers* 2018; 33: 215-221.

24 Vischioni B, Oudejans JJ, Vos W, Rodriguez JA, Giaccone G. Frequent overexpression of aurora B kinase, a novel drug target, in non-small cell lung carcinoma patients. *Mol Cancer Ther* 2006; 5: 2905-2913.

25 Takeshita M, Koga T, Takayama K, Ijichi K, Yano T, Maehara Y *et al*. Aurora-B overexpression is correlated with aneuploidy and poor prognosis in non-small cell lung cancer. *Lung Cancer* 2013; 80: 85-90.

26 Lampson MA, Renduchitala K, Khodjakov A, Kapoor TM. Correcting improper chromosome-spindle attachments during cell division. *Nat Cell Biol* 2004; 6: 232-237.

27 Liang C, Zhang Z, Chen Q, Yan H, Zhang M, Zhou L *et al*. Centromere-localized Aurora B kinase is required for the fidelity of chromosome segregation. *J Cell Biol* 2020; 219.

28 Gregan J, Polakova S, Zhang L, Tolic-Norrelykke IM, Cimini D. Merotelic kinetochore attachment: causes and effects. *Trends Cell Biol* 2011; 21: 374-381.

29 Welburn JP, Vleugel M, Liu D, Yates JR, 3rd, Lampson MA, Fukagawa T *et al*. Aurora B phosphorylates spatially distinct targets to differentially regulate the kinetochore-microtubule interface. *Mol Cell* 2010; 38: 383-392.

30 Cimini D, Wan X, Hirel CB, Salmon ED. Aurora kinase promotes turnover of kinetochore microtubules to reduce chromosome segregation errors. *Curr Biol* 2006; 16: 1711-1718.

31 Meppelink A, Kabeche L, Vromans MJ, Compton DA, Lens SM. Shugoshin-1 balances Aurora B kinase activity via PP2A to promote chromosome bi-orientation. *Cell Rep* 2015; 11: 508-515.

32 Zhou L, Liang C, Chen Q, Zhang Z, Zhang B, Yan H *et al*. The N-Terminal Non-Kinase-Domain-Mediated Binding of Haspin to Pds5B Protects Centromeric Cohesion in Mitosis. *Curr Biol* 2017; 27: 992-1004.

33 Haarhuis JH, Elbatsh AM, van den Broek B, Camps D, Erkan H, Jalink K *et al*. WAPL-mediated removal of cohesin protects against segregation errors and aneuploidy. *Curr Biol* 2013; 23: 2071-2077.

34 Sherwood R, Takahashi TS, Jallepalli PV. Sister acts: coordinating DNA replication and cohesion establishment. *Genes Dev* 2010; 24: 2723-2731.

35 Kueng S, Hegemann B, Peters BH, Lipp JJ, Schleiffer A, Mechtler K *et al*. Wapl controls the dynamic association of cohesin with chromatin. *Cell* 2006; 127: 955-967.

36 Liu D, Vader G, Vromans MJ, Lampson MA, Lens SM. Sensing chromosome bi-orientation by spatial separation of aurora B kinase from kinetochore substrates. *Science* 2009; 323: 1350-1353.

37 Cimini D. Detection and correction of merotelic kinetochore orientation by Aurora B and its partners. *Cell Cycle* 2007; 6: 1558-1564.

38 Gazdar AF. Activating and resistance mutations of EGFR in non-small-cell lung cancer: role in clinical response to EGFR tyrosine kinase inhibitors. *Oncogene* 2009; 28 Suppl 1: S24-31.

39 Gerber DE. EGFR Inhibition in the Treatment of Non-Small Cell Lung Cancer. *Drug Dev Res* 2008; 69: 359-372.

40 Stewart EL, Tan SZ, Liu G, Tsao MS. Known and putative mechanisms of resistance to EGFR targeted therapies in NSCLC patients with EGFR mutations-a review. *Transl Lung Cancer Res* 2015; 4: 67-81.

41 Arao T, Fukumoto H, Takeda M, Tamura T, Saijo N, Nishio K. Small in-frame deletion in the epidermal growth factor receptor as a target for ZD6474. *Cancer Res* 2004; 64: 9101-9104.

42 Vargas-Rondón N, Villegas VE, Rondón-Lagos M. The Role of Chromosomal Instability in Cancer and Therapeutic Responses. *Cancers (Basel)* 2017; 10.

43 Bakhoum SF, Compton DA. Chromosomal instability and cancer: a complex relationship with therapeutic potential. *J Clin Invest* 2012; 122: 1138-1143.

44 Chunduri NK, Storchová Z. The diverse consequences of aneuploidy. *Nat Cell Biol* 2019; 21: 54-62.

45 Zhou C, Zhu Y, Lu B, Zhao W, Zhao X. Survivin expression modulates the sensitivity of A549 lung cancer cells resistance to vincristine. *Oncol Lett* 2018; 16: 5466-5472.

46 Kavallaris M, Kuo DY, Burkhart CA, Regl DL, Norris MD, Haber M *et al*. Taxol-resistant epithelial ovarian tumors are associated with altered expression of specific beta-tubulin isotypes. *J Clin Invest* 1997; 100: 1282-1293.

47 Engelman JA, Zejnullahu K, Mitsudomi T, Song Y, Hyland C, Park JO *et al*. MET amplification leads to gefitinib resistance in lung cancer by activating ERBB3 signaling. *Science* 2007; 316: 1039-1043.

48 McDermott U, Pusapati RV, Christensen JG, Gray NS, Settleman J. Acquired resistance of non-small cell lung cancer cells to MET kinase inhibition is mediated by a switch to epidermal growth factor receptor dependency. *Cancer Res* 2010; 70: 1625-1634.

49 Nurwidya F, Takahashi F, Murakami A, Kobayashi I, Kato M, Shukuya T *et al*. Acquired resistance of non-small cell lung cancer to epidermal growth factor receptor tyrosine kinase inhibitors. *Respir Investig* 2014; 52: 82-91.

50 Lee AF, Chen MC, Chen CJ, Yang CJ, Huang MS, Liu YP. Reverse epithelial-mesenchymal transition contributes to the regain of drug sensitivity in tyrosine kinase inhibitor-resistant non-small cell lung cancer cells. *PLoS One* 2017; 12: e0180383.

51 Tulchinsky E, Demidov O, Kriajevska M, Barlev NA, Imyanitov E. EMT: A mechanism for escape from EGFR-targeted therapy in lung cancer. *Biochim Biophys Acta Rev Cancer* 2019; 1871: 29-39.

52 Yochum ZA, Cades J, Wang H, Chatterjee S, Simons BW, O'Brien JP *et al*. Targeting the EMT transcription factor TWIST1 overcomes resistance to EGFR inhibitors in EGFR-mutant non-small-cell lung cancer. *Oncogene* 2019; 38: 656-670.

53 Zhu X, Chen L, Liu L, Niu X. EMT-Mediated Acquired EGFR-TKI Resistance in NSCLC: Mechanisms and Strategies. *Front Oncol* 2019; 9: 1044.

54 Redmond KL, Papafili A, Lawler M, Van Schaeybroeck S. Overcoming Resistance to Targeted Therapies in Cancer. *Semin Oncol* 2015; 42: 896-908.

55 Rajagopalan H, Lengauer C. Aneuploidy and cancer. *Nature* 2004; 432: 338-341.

56 Gao C, Furge K, Koeman J, Dykema K, Su Y, Cutler ML *et al*. Chromosome instability, chromosome transcriptome, and clonal evolution of tumor cell populations. *Proc Natl Acad Sci U S A* 2007; 104: 8995-9000.

57 Andersson DI, Slechta ES, Roth JR. Evidence that gene amplification underlies adaptive mutability of the bacterial lac operon. *Science* 1998; 282: 1133-1135.

58 Salgueiro L, Buccitelli C, Rowald K, Somogyi K, Kandala S, Korbel JO *et al*. Acquisition of chromosome instability is a mechanism to evade oncogene addiction. *EMBO Mol Med* 2020; 12: e10941.

59 Orr B, Talje L, Liu Z, Kwok BH, Compton DA. Adaptive Resistance to an Inhibitor of Chromosomal Instability in Human Cancer Cells. *Cell Rep* 2016; 17: 1755-1763.

60 Lengauer C, Kinzler KW, Vogelstein B. Genetic instabilities in human cancers. *Nature* 1998; 396: 643-649.

61 Bertran-Alamillo J, Cattan V, Schoumacher M, Codony-Servat J, Giménez-Capitán A, Cantero F *et al*. AURKB as a target in non-small cell lung cancer with acquired resistance to anti-EGFR therapy. *Nat Commun* 2019; 10: 1812.